Molecular Crystals and Liquid Crystals

Publication details, including instructions for authors and subscription information:
http://www.tandfonline.com/loi/gmcl20

# Numerical Study of Liquid Crystal-Induced Optical Singularities

V. Ilyina [a] & S. Subota [b]

[a] CED Group, School of Engineering Sciences, University of Southampton, Highfield, Southampton, U.K.

[b] Theoretical Physics Group, Physics Department, Kiev State Shevchenko University, Kiev, Ukraine

Version of record first published: 22 Sep 2006

To cite this article: V. Ilyina & S. Subota (2006): Numerical Study of Liquid Crystal-Induced Optical Singularities, Molecular Crystals and Liquid Crystals, 453:1, 275-291

To link to this article: http://dx.doi.org/10.1080/15421400600653761

*Mol. Cryst. Liq. Cryst.*, Vol. 453, pp. 275–291, 2006

ISSN: 1542-1406 print/1563-5287 online
DOI: 10.1080/15421400600653761

Taylor & Francis
Taylor & Francis Group

# Numerical Study of Liquid Crystal-Induced Optical Singularities

**V. Ilyina**
CED Group, School of Engineering Sciences, University of Southampton, Highfield, Southampton, U.K.

**S. Subota**
Theoretical Physics Group, Physics Department, Kiev State Shevchenko University, Kiev, Ukraine

*The self-action of a laser beam incident on a liquid crystal cell can cause the refracted beam to exhibit singularities in the optical wave field. We present here a self-consistent study of this phenomenon using a Finite Difference Time Domain (FDTD) solver for non-linear optical devices. The self-consistent liquid crystal director-optics FDTD method treats both the full three-dimensional spatial structures of the refracted beam and the director. This paper presents the algorithm and tests the method by examining the output from a incident Gaussian beam. We discuss quantitative differences between these results and the earlier work, and further investigate the short and long wavelength limits.*

**Keywords:** FDTD method; Freedericks transitions; liquid crystals; optical singularities



## 1. INTRODUCTION

Recently there has been a considerable interest in the liquid crystal community in the FDTD (Finite Difference Time Domain) method. In this method light propagation is treated by solving Maxwell's equations directly. This method is robust and accurate in applications where the modelling of complex multirefractional and non-linear optical problems on a wide variety of length scales is required. The

The authors would like to thank Prof. Tim Sluckin, Dr. Lee Hazelwood, Prof. Victor Reshetnyak and Prof. Simon Cox for useful discussions. Funding for V.I. was provided by a HEFCE Overseas Research Studentship and by a studentship from the School of Engineering Sciences in the University of Southampton.

Address correspondence to V. Ilyina, School of Engineering Sciences, University of Southampton, Highfield, Southampton, SO17 1BJ, U.K. E-mail: v.ilyina@soton.ac.uk

method yields full information on transmitted, reflected and scattered electromagnetic fields. It can successfully describe the multiple scattering and reflections which occur during the light-director interaction. Moreover, it appears to be more accurate and also sometimes more efficient than the previously standard stratified media approaches.

A number of research groups have now applied the FDTD method to liquid crystal problems [l–5]. Previous FDTD studies in liquid crystals have involved classical cells [1,2], scattering in textured liquid crystals [4] and diffraction gratings [3]. In all cases, however, the optical field responds to, but does not affect, the director field and therefore the optical properties of the medium itself.

By contrast, in this paper we use the FDTD method to treat a problem in non-linear optics. The problem is the birth of optical singularities in the far field of the Gaussian beam after it had interacted with a liquid crystal cell.

We consider a homeotropic liquid crystal cell illuminated with a Gaussian laser beam. If the intensity of the beam exceeds the threshold value, the optical Freedericksz transition occurs. The director distribution takes the form of a complex Gaussian-like multidimensional function. Therefore, the cell acts as a Gaussian lens. The phase shift between ordinary and extraordinary rays of the transmitted beam induced in this way gives birth to peculiarities in the far-field wavefront.

This problem has recently been the subject of a considerable interest. There have been both experimental and theoretical studies of scenarios of the birth of singularities [6–10]. However, there have been no self-consistent studies of the phenomenon. This paper demonstrates that taking into account the feedback between light and the director considerably changes the position of the observed singularity and allows us to calculate it more accurately.

The layout of this paper is as follows. Section 2 analyzes the director distribution induced by the laser beam. The dynamic solutions to the director equation are considered. The dynamic solution combined with the FDTD algorithm allows the self-consistent algorithm to be implemented. In Section 3 we present far field calculations. We find that the edge optical singularity can be observed in the far-field. In Section 4 the results are compared with the non self-consistent approach. In Section 5 we discuss the results and consider long and short wave limits. Finally, Section 6 draws the conclusions.

## 2. DIRECTOR REORIENTATION INDUCED BY A GAUSSIAN LASER BEAM

Let us consider a nematic liquid crystal cell illuminated by a Gaussian laser beam. The cell is shown in Figure 1.

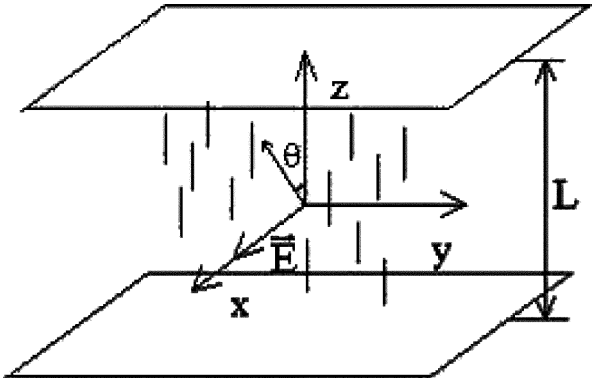


**FIGURE 1** The system geometry for the homeotropic liquid crystal illuminated by the Gaussian light beam polarised along $x$-axis.

Here $L$ is the width of the cell, polarisation of the incident electric field E is along $x$-axis and $\theta$ is the angle between the disturbed director and $z$-axis. The initial distribution of the director is homeotropic and we assume the infinite anchoring at the surfaces. The intensity of incident light is given by the Gaussian function:

$$I = I_0 \exp^{-\frac{x^2+y^2}{R^2}}, \tag{1}$$

where $I_0$ is the maximum intensity and $R$ is the semiwidth of the beam.

In the given geometry the director profile can be described by a vector **n** with the following components:

$$\mathbf{n} = [\sin\theta(x,y,z), 0, \cos\theta(x,y,z)]. \tag{2}$$

The free energy function for this geometry can be written as:

$$F = \frac{K}{2}\int(\theta_x'^2 + \theta_y'^2 + \theta_z'^2)\mathrm{d}V - \frac{1}{c}\int I(x,y)n_\tau \mathrm{d}V, \tag{3}$$

where $K$ is the elastic constant, $c$ is the speed of light in free space and

$$n_r = \frac{n_0}{\sqrt{1-\beta\sin^2\theta(x,y,z)}}$$

and $\beta = 1 - (n_0^2/n_e^2)$, where $n_0$ and $n_e$ are ordinary and extraordinary indices respectively.

Using the free energy (3) it is possible to write down the Ginzburg-Landau time-dependent equation for the director:

$$\gamma_1 \frac{\partial \theta}{\partial t} = K\left(\frac{\partial^2 \theta}{\partial x^2} + \frac{\partial^2 \theta}{\partial y^2} + \frac{\partial^2 \theta}{\partial z^2}\right) + \frac{n_0 \beta \bar{I}_0 e^{-\frac{x^2+y^2}{R^2}}}{c} \frac{\sin\theta\cos\theta}{(1-\beta\sin^2)^{3/2}} \tag{4}$$

In this equation $\gamma_1$ is the viscosity of a liquid crystal and $\tilde{I}_0$ is a time averaged value of intensity in the middle of the cell. It must be calculated from Maxwell's equations inside the liquid crystal. For the geometry of the problem they are:

$$\frac{\partial D_x}{\partial t} = -\frac{\partial H_y}{\partial z}, \tag{5}$$

$$\frac{\partial H_x}{\partial t} = -\frac{1}{\mu}\frac{\partial E_z}{\partial y}, \tag{6}$$

$$\frac{\partial H_y}{\partial t} = \frac{1}{\mu}\left(\frac{\partial E_z}{\partial x} - \frac{\partial E_x}{\partial z}\right). \tag{7}$$

Before solving Eqs. (5–7), $E_x$ and $E_z$ must be found from

$$\mathbf{E} = \hat{\varepsilon}^{-1}\mathbf{D}, \tag{8}$$

where

$$\hat{\varepsilon} = \varepsilon_0 \begin{pmatrix} n_e^2 \sin^2\theta + n_0^2 \cos^2\theta & 0 & (n_e^2 - n_0^2)\sin\theta\cos\theta \\ 0 & n_0^2 & 0 \\ (n_e^2 - n_0^2)\sin\theta\cos\theta & 0 & n_e^2\cos^2\theta + n_0^2\sin^2\theta \end{pmatrix} \tag{9}$$

The steady state value of Poynting vector in the middle of the cell gives the intensity $\tilde{I}_0$ as described in [11]. This value is then substituted into Eq. (4). Then Eqs. (4–7) are solved using the self-consistent algorithm described in detail for the optical Freedericksz transition in one dimension in [11]. The only distinct difference and complication with respect to the one dimensional case are the boundary conditions for Eq. (4).

The conditions in $z$ are easily derived from the strong anchoring conditions:

$$\theta(x,y,z=0) = 0, \quad \theta(x,y,z=L) = 0. \tag{10}$$

The boundary conditions in $x$ and $y$ must read

$$\theta(x \to \pm\infty, y, z) = 0, \quad \theta(x, y \to \pm\infty, z) = 0. \tag{11}$$

As the computational domain can not be extended to infinity, some approximation must be used to avoid these conditions.

Let us consider the case when the beam semiwidth $R$ is the same order of magnitude as the cell thickness $L$. We found from numerical experiments that in this case the computational domain as large as $10R$ in $x$ and $y$ direction is enough to minimize the boundary effect.

$$\theta(x = \pm 5R, y, z) = 0. \tag{12}$$

Due to the symmetry of the problem, the $y$ direction would be equivalent to the $x$ direction and therefore, the boundary conditions for $y$ read

$$\theta(x, y = \pm 5R, z) = 0. \tag{13}$$



Let us note that the choice of these boundary conditions, in principle, changes the symmetry of the beam from circular to square. However, in the cases considered here, the boundaries have been placed far enough from the periphery of the beam to ensure that they do not change the symmetry of the final result. We now nondimensionalize Eq. (4) by introducing the following variables:

$$\rho_1 = \frac{x}{L}, \tag{14}$$

$$\rho_2 = \frac{y}{10R}, \tag{15}$$

$$\rho_3 = \frac{z}{10R}, \tag{16}$$

$$\tau = \frac{K}{L^2 \gamma_1} t, \tag{17}$$

We also nondimensionalise the intensity inside the cell with respect to a value of the threshold intensity:

$$I_{\text{th}} = \frac{Kc\pi^2 (1 + \frac{L}{\pi R})^2}{n_0 \beta L^2} \tag{18}$$

which was found using the steady state analysis.

$$\tilde{I}_1 = \frac{\tilde{I}_0}{I_{\text{th}}} = \frac{\tilde{I}_0 n_0 \beta L^2}{Kc\pi^2 (1 + \frac{L}{\pi R})^2}. \tag{19}$$

Now Eq. (4) reads

$$\frac{\partial \theta}{\partial \tau} = \frac{L^2}{(10R)^2} \left( \frac{\partial^2 \theta}{\partial \rho_1^2} + \frac{\partial^2 \theta}{\partial \rho_2^2} \right) + \frac{\partial^2 \theta}{\partial \rho_3^2} + \tilde{I}_1 \left( 1 + \frac{L}{\pi R} \right)^2 e^{-(10)^2 (\rho_1^2 + \rho_2^2)} \times \frac{\pi^2 \sin\theta \cos\theta}{(1 - \beta \sin^2 \theta)^{3/2}}. \tag{20}$$

This equation describes the Freedericksz transition, which occurs when $\tilde{I}_1 = 1$. One can see that, as $R$ and $L$ have the same order of magnitude, $L^2/(10R)^2 \sim 10^{-2}$ and therefore, the impact of derivatives over $\rho_1$ and $\rho_2$ in Eq. (20) is negligible. We have carried out numerical tests to make sure this is indeed the case. However, tests have shown that if the beam is narrow, e.g., $R << L$, a much larger computational domain is needed to minimize the effect of boundaries.

Another interesting observation can be made from Eq. (20). It is easy to see that if $R \to \infty$, Eq. (20) reduces to an equation for a one dimensional Freedericksz transition. The threshold in this case will therefore coincide with the threshold for a one dimensional case. As the beam becomes narrower, the transition value increases as was predicted earlier.



## 3. FAR-FIELD ANALYSIS

Equation (20) has been solved consistently with Maxwell's Eqs. (5–7) using a 2d self-consistent algorithm. This algorithm was described in detail in [11]. The solutions provide the director distribution inside the cell and the field distribution both inside the cell and at the exit of the cell.

In order to find the far-field distribution we follow the analysis by Kreminskaya *et al.* in [7] for the Gaussian lens.

A focussing Gaussian lens can be described in terms of the transmission index [7]:

$$T(x,y) = T_0(x,y)\exp\left[i2\pi\exp\left(-\frac{x^2+(y^2)}{2a}\right)\right], \tag{21}$$

where $T_0$ is the transparency coefficient, which is the same as the transmission coefficient in the FDTD method. It was shown in [7] that the focal length for this lens is given by:

$$f = \left(\frac{\sqrt{2}a}{\omega}\right)^2 z_\omega/2\pi \simeq 0.16\left(\frac{\sqrt{2}a}{\omega}\right)^2 z_\omega, \tag{22}$$

where $z_\omega = \pi\omega^2/\lambda$ and $\omega = \sqrt{2}R$. The role of the focal distance in determining the phase singularities will be clarified later.

Beyond the lens the beam is a product of $U(x,y)T(x,y)$ where $U(x,y)$ is the initial beam amplitude distribution at $z = 0$. Then the complex field amplitude of the beam cross-section in the $z$-plane is denned as [7]:

$$U(x_1,y_1,z) \sim \iint \mathrm{d}x\mathrm{d}y U(x,\ y)T(x,y)\exp\left(i\frac{z_\omega}{z}[(x-x_1)^2+(y-y_1)^2]\right). \tag{23}$$

This equation is obtained from the Huygens-Fresnel theory in the Fresnel approximation for $z >> x, y$. The FDTD algorithm does not directly predict the transmission function $T(x, y)$. Rather it provides the field at the exit from the cell is represented by 2d complex matrix $U_{i,j}$ where $i, j$ correspond to the $x, y$ locations. By analogy with the Gaussian lens one can write the far field as:

$$U_{i_1,j_1}(z) \sim \sum_i \sum_j U_{i,j} \exp\left(i \frac{z_\omega}{z} [(x_i - x_{i_1})^2 + (y_j - y_{j_1})^2]\right) \Delta x_i \Delta y_j, \quad (24)$$

where $\Delta x_i$ and $\Delta y_j$ are cell dimensions in the numerical algorithm.

Using the FDTD method the field distribution beyond the cell has been obtained for the several values of $z$. Just after the cell the beam preserves the Gaussian amplitude distribution, but acquires Gaussian phase distribution as shown in Figures 2–3. When the distance $z$ increases, the central part of the beam is focussing and forms a waist with radius $R_0 = 0.4\,\mu\text{m}$ at $z \sim 0.22 z_\omega$ distance from the cell and it is accompanied by a circular shallow valley as shown in Figure 4. The focal length is given by Eq. (22), where for the given intensity $a = 11.5\,\mu\text{m}$. Figure 5 shows that the phase distribution has a flat top ledge. The beam soon reaches the pre-dislocation stage at $z = 0.3 z_\omega$: the valley bottom is nearly zero and the height of the phase ledge tends to $\pi$ as Figures 6–7 show.

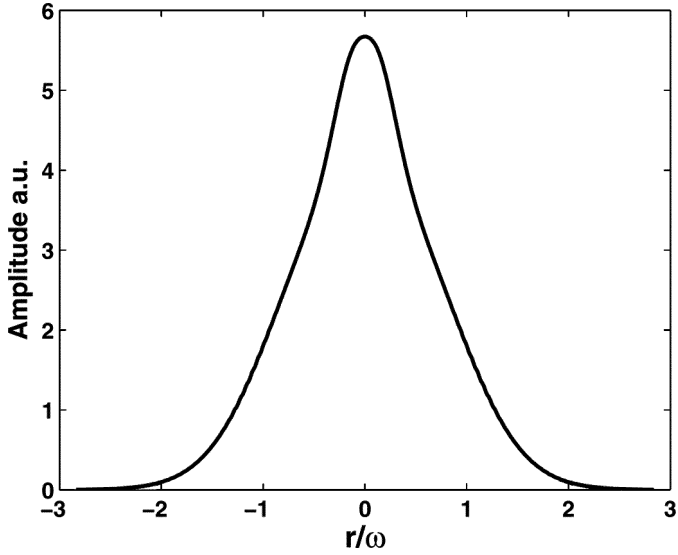


**FIGURE 2** Amplitude of the beam at the exit from the cell.

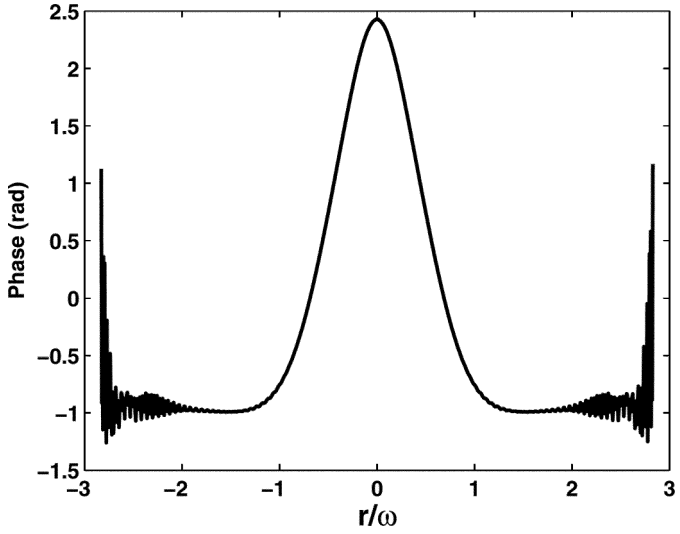


**FIGURE 3** Phase of the beam at the exit from the cell.

By further increasing $z$, the bottom of the circular valley becomes exactly zero and the phase ledge transforms to a circular $\pm\pi$ phase jump with vertical walls (Figs. 8, 9). At $z = 0.324z_\omega$ the circular edge

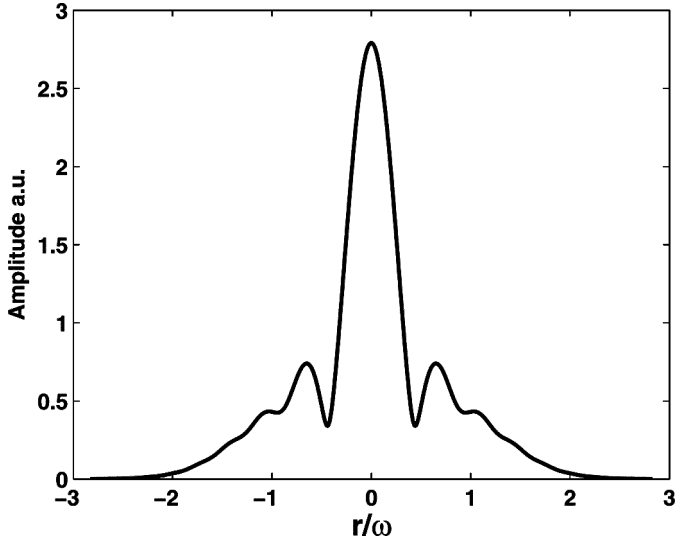


**FIGURE 4** Amplitude of the beam at $z \sim 0.22z_\omega$ Beam is focussed.

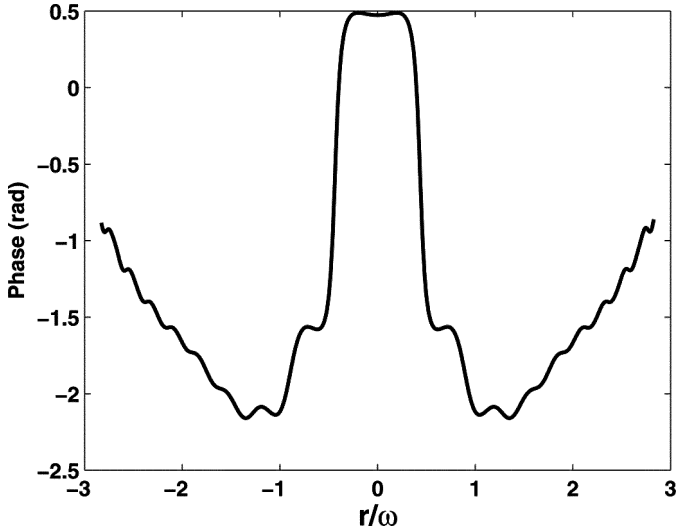


**FIGURE 5** Phase of the beam at $z \sim 0.22z_\omega$. The phase has a flat ledge in the middle of the distribution.

dislocation with radius $r \sim 0.5\omega$ is born. Its dislocation strength equals unity according to the theory [12]. It is interesting to note that the distance of the dislocation birth $z = 0.324z_\omega$ exceeds the distance of the waist formation $z = 0.3z_\omega$, which in turn exceeds the focal length

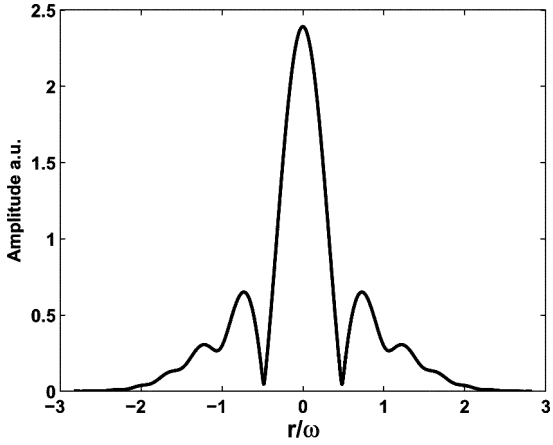


**FIGURE 6** Amplitude at $z = 0.3z_\omega$ – pre-dislocation stage: the valley bottom is nearly zero.

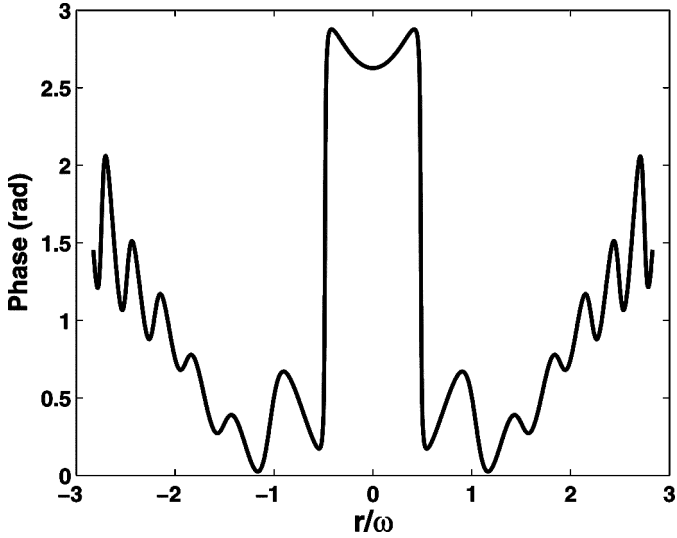


**FIGURE 7** Phase at $z = 0.3z_\omega$ – pre-dislocation stage: the height of the phase ledge tends to $\pi$.

$f = 0.22z_\omega$. Hence, the circular edge dislocation appears when the focussing beam starts to diverge. The dislocation disappears immediately with the smallest distance increase (physically on a length of

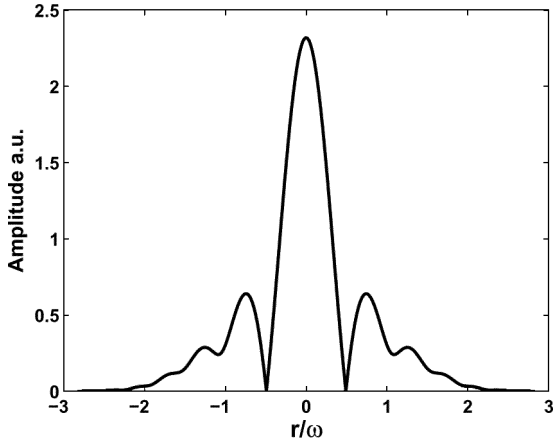


**FIGURE 8** Amplitude at $z = 0.324z_\omega$ is exact zero at $r \sim 0.5\omega$ – edge dislocation is born.

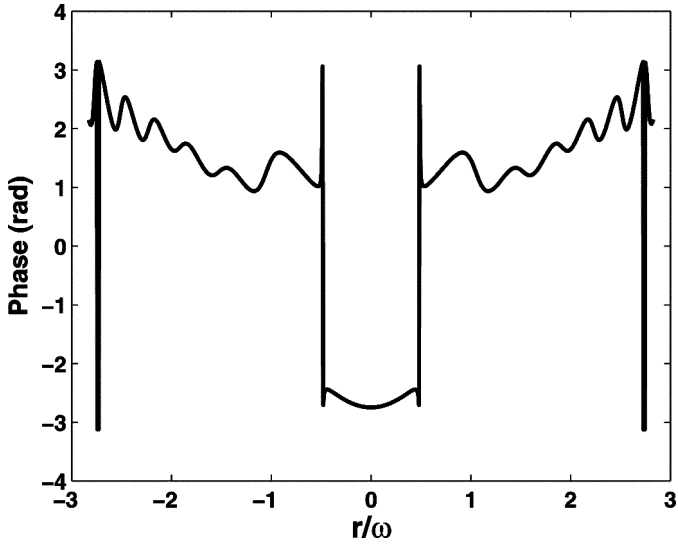


**FIGURE 9** Phase at $z = 0.324z_\omega$ is experiencing a $2\pi$ jump.

the wave length scale). At this distance $z \sim 0.33z_\omega$ the valley bottom becomes nonzero and the phase jump transforms to a smooth ledge with slanted walls as shown in Figures 10 and 11.

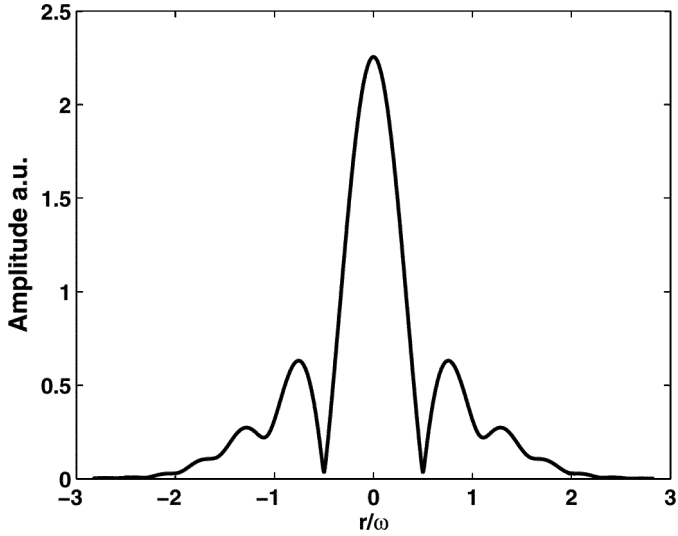


**FIGURE 10** Amplitude at $z \sim 0.33z_\omega$ – disappearance of dislocation.

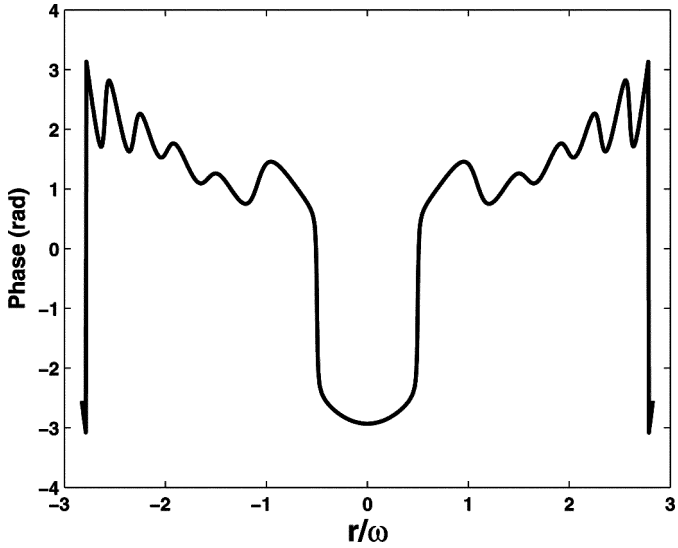


**FIGURE 11** Phase at $z \sim 0.33z_\omega$ – disappearance of dislocation.

## 4. COMPARISON WITH THE NON SELF-CONSISTENT APPROACH

The previous section has presented results obtained using the self-consistent FDTD algorithm. We now compare them with the results from the non-self-consistent approach. These calculations for the same liquid crystal system were carried out in two steps. First, the steady state distribution of the director under the constant intensity was calculated from static equation without taking into account the coupling with the beam. At the second step a paraxial approximation was used to study beam propagation within the cell and to predict the field distribution at the exit from the cell. From these calculations a singularity was predicted at the distance of $z = 0.245z_\omega$; a discrepancy of 24% as compared to the self-consistent result of $z = 0.324z_\omega$. This difference increases for a higher anisotropic liquid crystal with refractive indices $n_0 = 1.54$, $n_e = 1.76$. For this case, the singularity was observed at $z = 0.102z_\omega$. For the non-self-consistent algorithm this distance was $z = 0.067z_\omega$. The discrepancy from the self-consistent results is now about 34%.

The difference in results can be explained in the following way. In the non-self-consistent approach the incident intensity was assumed to equal to the internal intensity. However, when calculated

self-consistently, the internal intensity is different from the incident intensity and it is always smaller as some intensity is reflected by the cell boundaries.

The increasing difference in the case of a highly anisotropic cell is not only due to the lack of self-consistency, but also due to limitations in the paraxial approximation. The accuracy of this approximation decreases with increasing the optical anisotropy.

We thus conclude that the self-consistent algorithm allows one to calculate the position of singularities more accurately. It also allows calculations in different wave-length limits, while the paraxial approximation used in the non-self-consistent approach can only consider wavelengths, which are short in comparison to the thickness of the cell $L$. Next section will investigate these limits.



## 5. SHORT AND LONG WAVE-LENGTH LIMIT

The non-self-consistent approach allows the transition to be calculated only for wavelengths much shorter than the cell thickness. One of the advantages of the FDTD approach is that the calculations are also possible for long wavelengths.

Let us introduce the parameter $b$ that defines the ratio of the cell thickness $L$ to the wavelength $\lambda$

$$b = \frac{L}{\lambda}. \tag{25}$$

Large values of $b$ correspond to the limit where the paraxial approximations is valid. The smaller the value of $b$, the less accurate are the paraxial approximations results.

Let us consider the range of $b = [0.1, 10]$. FDTD calculations have been carried out for the same system and numerical parameters as above, but with different values of $\lambda$. Let us first look at the phase of the beam at the exit from the cell. Figure 12 shows phase distribution in the $xy$ plane for four different values of $b$. The dashed line corresponds to $b = 10$ and one can see pronounced Gaussian variation of the phase. In this case the beam will focuss after the cell and then diverge, and the singularity will be observed. It was found that for this $b$ the singularity is born at $z = 0.680 z_\omega$. Further in Figure 12 circled and crossed lines correspond to $b = 6$ and $b = 2$ respectively. One can observe that decreasing $b$ decreases the phase lag between the center of the beam and its wings. This corresponds to smaller semi-width of the director distribution $a$. Therefore, according to Eq. (22) the focal distance in units of $z_\omega$ will increase. This means that the

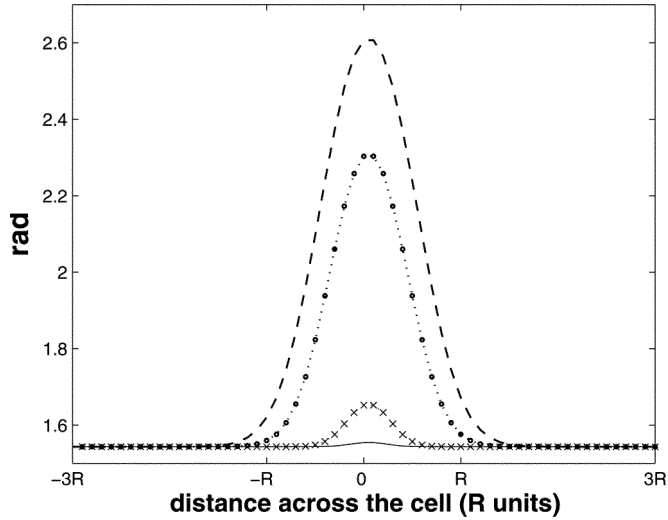


**FIGURE 12** The beam phase at the exit from the cell for different values of $b$. Dashed line-$b = 10$, circled line-$b = 6$, crossed line-$b = 2$, solid line-$b = 0.1$.



beam will focuss and diverge further from the cell, and therefore, the singularity will be observed further in units $z_\omega$ too. It was found that for $b = 6$ the singularity is observed at $z = 0.947 z_\omega$ and for $b = 2$ the singularity is observed at $z = 1.638 z_\omega$. Finally, the solid line in Figure 12 corresponds to $b = 0.1$. Here hardly any disruption of a wavefront is observed. Calculations showed that the beam did not focuss and therefore did not diverge. The singularity has disappeared. In fact, as soon as $b$ becomes less than 1 the singularity cannot be observed. The beam does not see the liquid crystal cell and therefore, the wavefront does not change. One might think that singularity disappears to the infinity. However, this is not the case. The distance to the singularity grows only in units of $z_\omega$. However, $z_\omega = \pi\omega^2/\lambda$ and obviously decreases with increasing $\lambda$. This decrease is faster than growth of the distance in units of $z_\omega$. Figure 13 confirms this fact by showing both function $1/z_\omega$ and $z$ plotted against $b$.

Figure 14 shows how the physical distance to singularity changes with decreasing $b$. One can observe the transition-like curve, with the singularity being observed closer and closer to the cell, until in eventually disappears at $b = 1$.

The full list of physical and numerical parameters used in the calculations is given in Table 1.

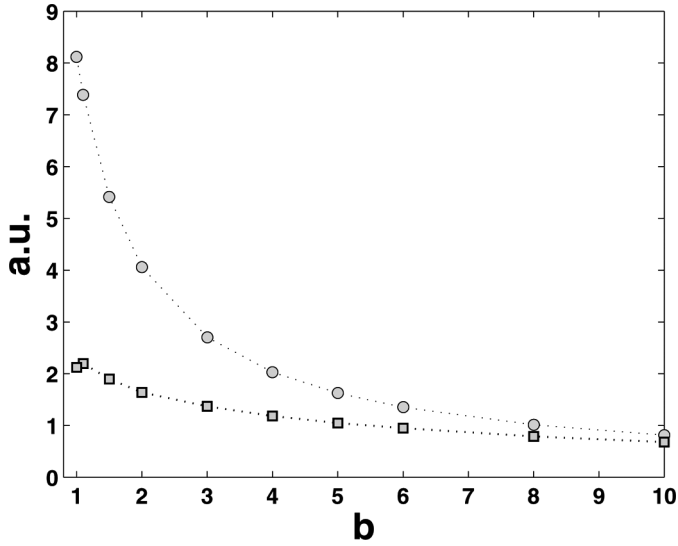


**FIGURE 13** Functions $1/z_\omega$ (circles) and distance to singularity in $z_\omega$ units $z$ (squares) are plotted against $b$. One can see that $1/z_\omega$ decreases faster than $z$ and therefore, physical distance decreases with decreasing $b$.

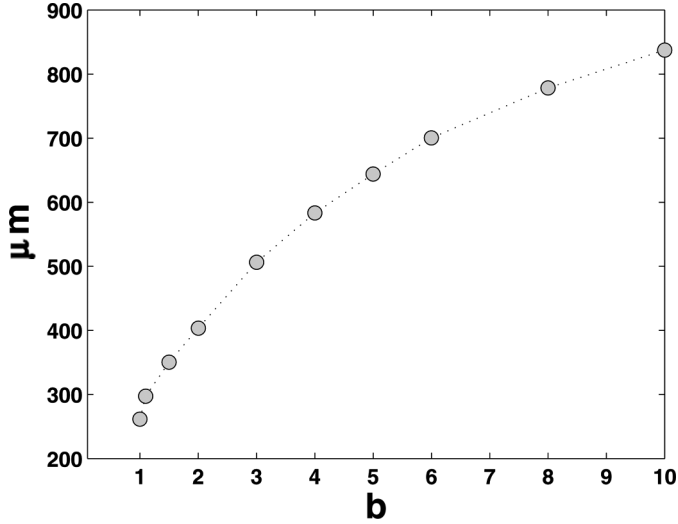


**FIGURE 14** Physical distance to singularity versus $b$. Singularity disappears at $b < 1$.

**TABLE 1** Numerical and Physical Parameters Used in Simulation

| Meaning | Parameter | Value |
|---|---|---|
| No. of time steps | $N$ | 30000–40000 |
| Spatial grid size | $dz = \lambda/66$ | 9.6 nm |
| Spatial grid sizes | $dx = dy$ | 800 nm |
| Time grid size | $dt = dz/c$ | $3.2 \times 10^{-17}$ sec |
| Liquid crystal cavity relaxation time | $\tau_f = Ndt$ | $9.6 \times 10^{-13}$ sec |
| Liquid crystal extraordinary refractive index | $n_e$ | 1.53 |
| Liquid crystal ordinary refractive index | $n_0$ | 1.47 |
| Dielectric anisotropy | $\varepsilon_a$ | 0.18 |
| Frank-Oseen elastic constant | $K$ | $10^{-12}$ N |
| Viscosity parameter | $\gamma_1$ | 0.08 Pa·sec |
| Light wavelength in free space (main value) | $\lambda$ | 633 nm |
| Thickness of cell (main value) | $L$ | 20 μm |
| Width of the beam | $\omega$ | 14 μm |
| Threshold intensity | $I_{th}$ | 10.8 kW/cm$^2$ |
| Incident intensity | $I$ | $1.3I_{th}$ |

## 6. CONCLUSIONS

We have used the FDTD method for modelling a three-dimensional problem of the Freedericksz transition induced by a Gaussian beam and the birth of the optical singularities in the far-field of the beam with the initially smooth wavefront.

The FDTD algorithm has allowed us to study optical fields inside the cell and at the exit from the cell. We found that after the cell the beam focusses and then diverges again. At the distance from the cell corresponding to diverging of the beam, the edge optical singularity has been observed. This result has been compared with the result obtained using the non-self-consistent approach. It was found that two results are different, and the difference increases with the optical anisotropy.

Different wave-lengths limits were also investigated, which is not possible for the non-self-consistent approach. We found that in the very long wavelength limit the singularity disappears. Similar effect is observed when decreasing the size of the cell. The ratio of $L/\lambda$, at which the singularity disappears was found to be equal to 1. The results have shown that for $L/\lambda < 1$ the phase lag induced by the cell is not large enough to cause the distortion of the wavefront.

One of the possible extensions to the results this paper is to replace the Ginzburg-Landau equation in the self-consistent algorithm by the Ericksen-Leslie equations. This would allow us to take into account hydrodynamical effects such as back-flow. Thus, extra coupling, now

director-hydrodynamics, will be introduced in the problem. This might considerably change the relaxation process. However, we believe that the final equilibrium will not be changed.

Another interesting extension would be to consider how the position of the singularity depends on the optical anisotropy $\Delta n$. Preliminary calculations show that change of the optical anisotropy has a considerable effect on the position of the singularity, bringing it closer to the cell. However, what the true dependence is and whether there is any influence on the type of singularity from the value of optical anisotropy remains an interesting open questions. We believe that highly anisotropic liquid crystals may induce more complex singularities. This is because the sharp variations of the director in the *xy* plane may induce the phase profile that is not smooth. This will influence the far-field observations dramatically. In this case, however, the accuracy would require higher order discretisation schemes, as used in [3].

We believe the three-dimensional self-consistent FDTD solver presented is this paper can be used a an accurate and robust tool for studying nonlinear interactions of light and liquid crystal media.

## REFERENCES

[1] Witzigmann, B., Regli, P., & Fichtner, W. (1998). *J. Opt. Soc. Am.*, *A15*, 753–757.
[2] See e.g., Kriezis, Em. E. & Elston, S. J. (2000). *Opt. Com.*, *165*, 99–105.
[3] See e.g., Bos, P. & Wang, B. (2003). *J. Opt. Soc. Am. A*, *2*, 2123–2130.
[4] Hwang, D. K. & Rey, A. D. (2005). *Liq. Cryst.*, *32*, 483–497.
[5] Ilyina, V., Cox, S. J., & Sluckin, T. J. (2004). *Mol. Cryst. Liq. Cryst.*, *422*, 1–10.
[6] Ilyenkov, A. V., Khiznyak, A. I., Kreminskaya, L. V., Soskin, M. S., & Vasnetsov, M. V. (1996). *Appl. Phys. B*, *62*, 465–471.
[7] Kreminskaya, L. V., Soskin, M. S., & Khiznyak, A. I. (1998). *Optics Com.*, *145*, 377–384.
[8] Arakelyan, S. M., Darbin, S. D., & Shen, I. F. (1982). *Light-Induced Orientational Effects in Nematics: Laser Interaction with Liquid Crystals – Interuniversity Scientific Journal*, (in Russian).
[9] Pishnyak, O. P., Reznikov, Yu. A., & Vasnetsov, M. V. (1998). *Mol. Cryst. Liq. Cryst.*, *324*, 25–30.
[10] Subota, S., Reshetnyak, V., & Soskin, M. S. (2002). *Mol. Cryst. Liq. Cryst.*, *375*, 481–490.
[11] Ilyina, V., Sluckin, T., & Cox, S. (2006). *Accepted by Optics Communications*.
[12] Nye, J. F. & Berry, M. (1974). *Proc. R. Soc. Lond.*, *336*, 165–190.